Carbon monoxide differentially inhibits TLR signaling pathways by regulating ROS-induced trafficking of TLRs to lipid rafts

Kiichi Nakahira,[1] Hong Pyo Kim,[1] Xue Hui Geng,[2] Atsunori Nakao,[3] Xue Wang,[1] Noriko Murase,[3] Peter F. Drain,[2] Xiaomei Wang,[1] Madhu Sasidhar,[4] Elizabeth G. Nabel,[5] Toru Takahashi,[6] Nicholas W. Lukacs,[7] Stefan W. Ryter,[1] Kiyoshi Morita,[6] and Augustine M.K. Choi[1]

[1]Division of Pulmonary, Allergy and Critical Care Medicine, [2]Department of Cell Biology and Physiology, and [3]Department of Surgery, University of Pittsburgh School of Medicine, Pittsburgh, PA 15213
[4]Section of Pulmonary and Critical Care Medicine, Yale University School of Medicine, New Haven, CT 06520
[5]National Heart, Lung, and Blood Institute, National Institutes of Health (NIH), Bethesda, MD 20892
[6]Department of Anesthesiology and Resuscitology, Okayama University Medical School, Okayama-shi 700-8558, Japan
[7]Department of Pathology, University of Michigan Medical School, Ann Arbor, MI 48109

Carbon monoxide (CO), a byproduct of heme catabolism by heme oxygenase (HO), confers potent antiinflammatory effects. Here we demonstrate that CO derived from HO-1 inhibited Toll-like receptor (TLR) 2, 4, 5, and 9 signaling, but not TLR3-dependent signaling, in macrophages. Ligand-mediated receptor trafficking to lipid rafts represents an early event in signal initiation of immune cells. Trafficking of TLR4 to lipid rafts in response to LPS was reactive oxygen species (ROS) dependent because it was inhibited by diphenylene iodonium, an inhibitor of NADPH oxidase, and in gp91^{phox}-deficient macrophages. CO selectively inhibited ligand-induced recruitment of TLR4 to lipid rafts, which was also associated with the inhibition of ligand-induced ROS production in macrophages. TLR3 did not translocate to lipid rafts by polyinosine-polycytidylic acid (poly(I:C)). CO had no effect on poly(I:C)-induced ROS production and TLR3 signaling. The inhibitory effect of CO on TLR-induced cytokine production was abolished in gp91^{phox}-deficient macrophages, also indicating a role for NADPH oxidase. CO attenuated LPS-induced NADPH oxidase activity in vitro, potentially by binding to gp91^{phox}. Thus, CO negatively controlled TLR signaling pathways by inhibiting translocation of TLR to lipid rafts through suppression of NADPH oxidase–dependent ROS generation.

CORRESPONDENCE
Augustine M.K. Choi:
choiam@upmc.edu

Abbreviations used: CO, carbon monoxide; CTx, cholera toxin; DPI, diphenylene iodonium; GM1, glycosphingolipid 1; HO, heme oxygenase; IP-10, IFN-γ–inducible protein 10; IRF-3, IFN regulatory factor 3; MAPK, mitogen-activated protein kinase; MβCD, methyl-β-cyclodextrin; MDC, monodansylcadaverine; NAC, *N*-acetyl-L-cysteine; PAMP, pathogen-associated molecular pattern; poly(I:C), polyinosine-polycytidylic acid; RANTES, regulated upon activation, normal T expressed, and presumably secreted; ROS, reactive oxygen species; TLR, Toll-like receptor; TRAF, TNF receptor–associated factor; TRIF, TIR domain–containing adaptor-inducing IFN-β.

Carbon monoxide (CO) arises physiologically in cells during the oxidative catabolism of heme by heme oxygenase (HO) enzymes (1). HO-1, an inducible isoform of HO, provides a protective response to injury associated with proapoptotic stimuli or inflammation (1). Both mice and humans deficient in HO-1 expression have a phenotype of an increased inflammatory state (2–4). We have previously described that CO can not only suppress LPS-induced proinflammatory cytokine production, but also decrease mortality in a mouse model of sepsis (5, 6). We further showed that these antiinflammatory effects of CO are mediated by the mitogen-activated protein kinase (MAPK) pathway (5, 6). However, nothing is known regarding the effect of CO on upstream Toll-like receptor (TLR) signaling pathways.

TLRs are innate receptors critically involved in the initial phase of microbial detection (7). The recognition of distinct pathogen-associated molecular patterns (PAMPs) by TLRs activates signaling pathways that induce the expression of proinflammatory genes (7). Although the immune system of TLRs contributes to host defense, the TLRs have also been implicated in the pathogenesis of inflammatory human diseases (7, 8). To avoid inappropriate hyperresponses of the immune system,

K. Nakahira and H.P. Kim contributed equally to this work.
The online version of this article contains supplemental material.

the intensity and duration of TLR signaling require tight regulation (7, 8).

Plasma membranes of cells contain specialized microdomains called lipid rafts, which exert an important function in signal transduction of the immune system (9, 10). Several studies have demonstrated that membrane rafts play a key role in T cell and B cell activation by accumulating essential signaling molecules (9, 10). Recently, it has been apparent that lipid rafts are required not only for adaptive immune responses, but also for innate immune responses (10). TLR2 or TLR4 is recruited to membrane rafts by ligand or bacteria treatment (11, 12). Disruption of lipid rafts by methyl-β-cyclodextrin (MβCD) or nystatin inhibits proinflammatory cytokine production (11, 12).

Here we investigated how CO affects TLR signaling pathways in macrophages. CO negatively regulated TLR2, 4, 5, and 9 signaling pathways, but not TLR3. Although TLR4 translocated to lipid rafts after LPS stimulation and CO suppressed its recruitment, TLR3 did not translocate to lipid rafts and remained in the intracellular compartment after polyinosine-polycytidylic acid (poly(I:C)) stimulation in the absence or presence of CO. We demonstrated differential trafficking patterns of TLRs to lipid rafts. CO inhibits trafficking of not only TLRs but also of adaptor molecules, resulting in the suppression of downstream signaling pathways. Furthermore, we show that NADPH oxidase-dependent reactive oxygen species (ROS) production is involved in the translocation of TLR4 to lipid rafts by LPS, and that CO inhibits that trafficking by regulating NADPH oxidase activity.

RESULTS

Increased expression of TNF-α in HO-1$^{-/-}$ null mice

Because HO-1 is a well-known cytoprotective protein induced by inflammation or oxidative stress (1), we evaluated the physiological properties of HO-1 in vivo by using HO-1 null (HO-1$^{-/-}$) mice. We stained kidneys and livers for CI:A3-1 as an indicator of mouse monocytes or macrophages, and for TNF-α by immunohistochemistry under basal untreated conditions. We observed significant infiltration of macrophages and TNF-α expression around the convoluted tubules in the cortex of the kidney from HO-1$^{-/-}$ mice (Fig. 1, A and B). In contrast, immunohistochemical staining for macrophages and TNF-α was negligible in the kidney of wild-type (HO-1$^{+/+}$) mice (Fig. 1, C and D). In the livers from HO-1$^{-/-}$ mice (Fig. 1 E), marked accumulation of macrophages was observed in the portal vein accompanied with cellular infiltration in the interlobular septum as compared with in the liver from HO-1$^{+/+}$ mice (Fig. 1 G). Kupffer cells, which also can be stained by the CI:A3-1 marker, are likely to represent the increased staining observed in the sinusoid of the liver from HO-1$^{-/-}$ mice relative to that from HO-1$^{+/+}$ mice (Fig. 1, E and G). TNF-α expression was also markedly induced, consistent with localization of the macrophages in the liver from HO-1$^{-/-}$ mice (Fig. 1 F), as compared with liver from HO-1$^{+/+}$ mice (Fig. 1 H). In addition, increased staining for macrophages and expression of TNF-α was observed in the intestines from HO-1$^{-/-}$ mice compared with control mice (unpublished data). These results suggest that systemic inflammation is chronically increased in the HO-1$^{-/-}$ mice (2–4), consistent with the known antiinflammatory properties of HO-1 and the involvement of HO-1 in regulating the functions of monocyte/macrophages (13, 14).

Negative regulation of HO-1 in TLR signaling is mediated by CO

HO-1 is significantly induced by LPS (a ligand for TLR4) stimulation and has been shown to dampen the inflammatory effects of LPS-treated models (5, 13, 14). Therefore, we examined whether HO-1 could modulate the immune response in various TLR signaling pathways. HO-1–overexpressing

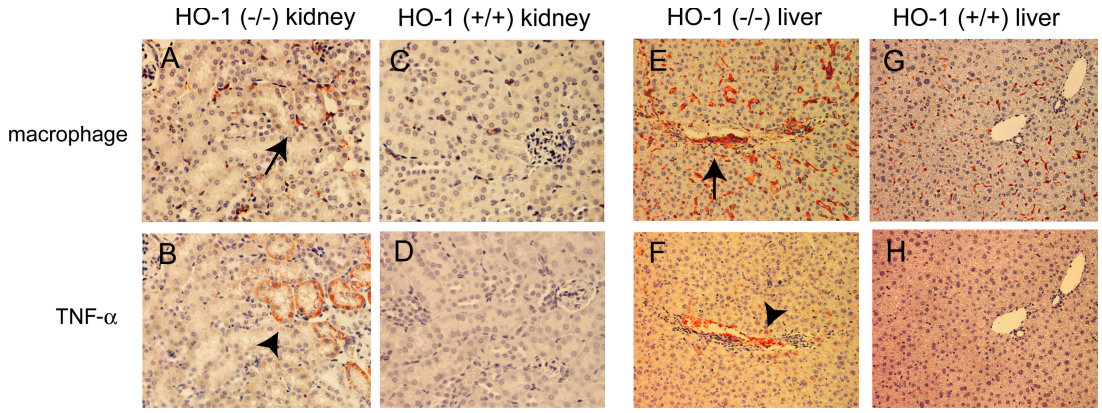

Figure 1. Expression of TNF-α and macrophages in the kidneys and livers of HO-1 null mice. Livers and kidneys were harvested from HO-1 null mice (HO-1$^{-/-}$; $n = 3$) or wild-type mice (HO-1$^{+/+}$; $n = 3$) under untreated conditions, and tissue sections were immunostained with anti–TNF-α or anti–CI:A3-1 for the detection of macrophages/monocytes. Representative light microscopic views are shown. Arrows and arrowheads indicate the influx of macrophages and TNF-α expression, respectively.

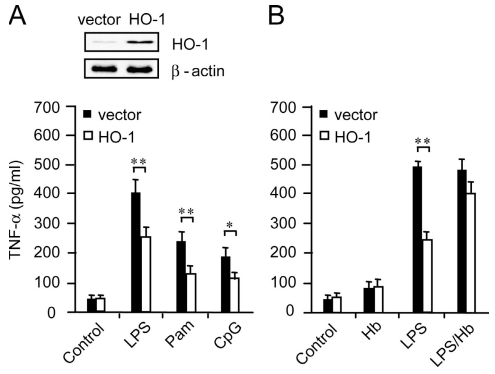

Figure 2. Effect of HO-1 overexpression on TLR ligand–induced TNF-α production in macrophages. (A) RAW 264.7 cells overexpressing HO-1 or control cells were treated with 100 ng/ml LPS, 100 ng/ml Pam, or 1 μM CpG for 1 h, and culture media were collected for TNF-α measurement. (B) The cells were pretreated with 5 μM of hemoglobin (Hb) for 30 min and stimulated with LPS for 1 h. TNF-α in culture media was measured by ELISA. *, $P < 0.05$ and **, $P < 0.01$ versus HO-1–overexpressing cells.

RAW 264.7 macrophages produced significantly less TNF-α than the control cells in response to LPS, Pam_3CSK4 (a ligand for TLR2), and CpG (a ligand for TLR9) (Fig. 2 A; references 5 and 6). However, when the HO-1–overexpressing cells were treated with LPS and hemoglobin, a scavenger of CO (14), the cells failed to inhibit LPS-induced TNF-α production (Fig. 2 B). These data suggest that the antiinflammatory effect of HO-1 on TLR signaling pathways in macrophages is mediated primarily by CO (5).

CO differentially inhibits TLR signaling

Because HO-1 inhibited TLR2, 4, and 9 ligand–induced TNF-α production (Fig. 2 A), and CO as a byproduct of heme catabolism by HO-1 was critically involved with the antiinflammatory effect of HO-1 (Fig. 2 B), we next investigated the effect of CO on various TLR ligand–induced cytokine production in RAW 264.7 cells (TLR ligands; TLR2, peptidoglycan or Pam_3CSK4 [Pam]; TLR3, double-stranded RNA poly(I:C); TLR4, LPS; TLR5, flagellin [Fla]; and TLR9, CpG). CO exposure significantly suppressed TLR2, 4, 5, and 9 ligand–induced TNF-α production (Fig. 3 A), which is similar to the effect of HO-1 observed in Fig. 2 A. However, CO did not affect poly(I:C)-induced TNF-α production (Fig. 3 A). As previously described, the effect of CO on LPS-induced cytokine production was dose dependent over a range of 50–500 ppm (5, 6); however, cytokine production by poly(I:C) was not affected by CO exposure at any of the doses (Fig. 3 B). To further confirm the effect of CO on macrophages, mouse peritoneal macrophages were stimulated with the TLR ligands in the presence or absence of CO. The effect of CO on TNF-α production in the mouse peritoneal macrophages was consistent with that observed in RAW 264.7 macrophages (Fig. 3, A and C). Because poly (I:C) is recognized not only by TLR3 but also by the helicase domain of MDA5 or RIG-I (15), we examined the relative role of TLR3 in poly(I:C)-induced cytokine production by using peritoneal macrophages from TLR3-deficient mice (*tlr3*$^{-/-}$). Consistent with previous results (16), poly(I:C)-induced TNF-α production in *tlr3*$^{-/-}$ macrophages was reduced to nearly background levels, relative to the poly (I:C)-induced TNF-α production observed in wild-type

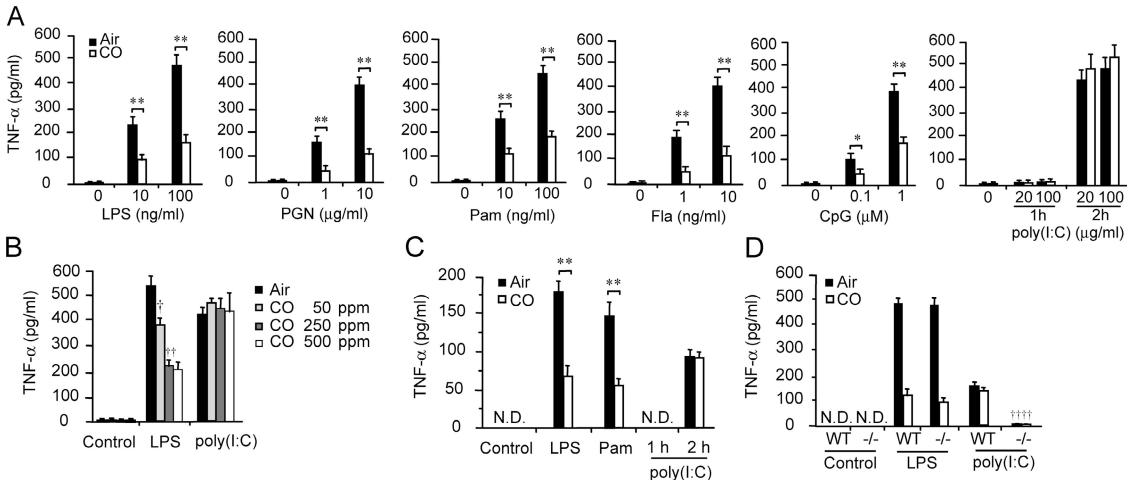

Figure 3. Effect of CO on TLR ligand–induced TNF-α production in macrophages. (A) RAW 264.7 cells were pretreated with 250 ppm CO for 2 h, followed by stimulation with the indicated concentrations of TLR ligands. Cell media were collected 1 or 2 h after the ligand treatment and TNF-α was measured by ELISA. *, $P < 0.05$ and **, $P < 0.01$ versus CO-treated cells. (B) Cells were treated with various concentrations of CO and stimulated with 100 ng/ml LPS or 20 μg/ml poly(I:C) for 1 or 2 h. TNF-α in the culture media was measured. †, $P < 0.05$ and ††, $P < 0.01$ versus LPS-treated control cells. (C) Mouse peritoneal macrophages were pretreated with 250 ppm CO for 2 h, followed by stimulation with TLR ligands for 1 or 2 h. Culture media were collected and TNF-α was measured by ELISA. **, $P < 0.01$ versus CO-treated cells. (D) Mouse peritoneal macrophages from wild-type (WT) mice or TLR3-deficient mice (−/−) were stimulated with 100 ng/ml LPS or 20 μg/ml poly(I:C) for 1 or 2 h, and TNF-α in culture media was measured by ELISA. ††, $P < 0.01$ versus poly(I:C)-stimulated wild-type cells.

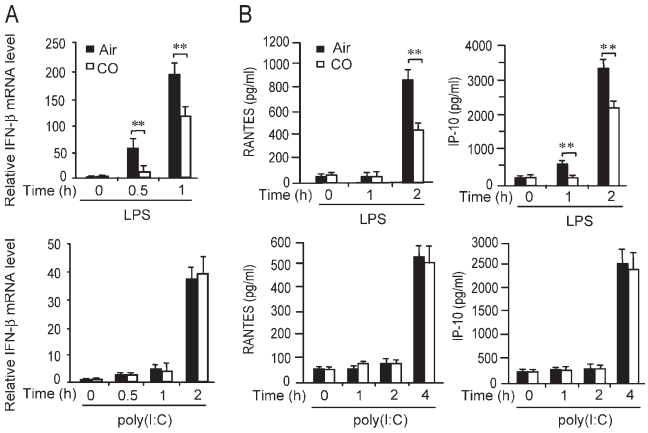

Figure 4. Effect of CO on IRF-3–related cytokine production in macrophages. (A) RAW 264.7 cells were treated with 100 ng/ml LPS or 20 μg/ml poly(I:C) in the absence or presence of CO, and their IFN-β mRNA expression at the indicated time points was analyzed by real-time RT-PCR. (B) IP-10 and RANTES production in culture media was analyzed by ELISA. **, $P < 0.01$ versus CO-treated cells.

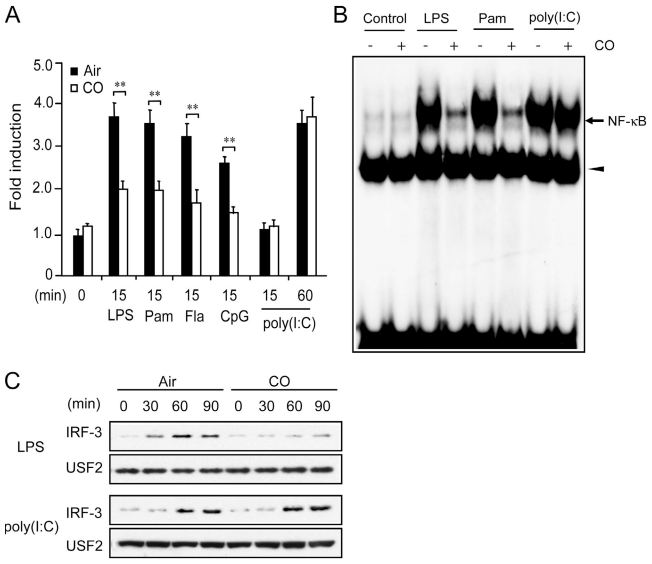

Figure 5. CO inhibits activation of NF-κB and nuclear translocation of IRF-3 by LPS, but not by poly(I:C). RAW 264.7 cells were stimulated with 100 ng/ml LPS, 100 ng/ml Pam, 10 ng/ml Fla, 1 μM CpG, and 20 μg/ml poly(I:C) in the presence or absence of CO. Nuclear protein was extracted for NF-κB activation assay or Western blot analysis. (A) NF-κB (p65) activation was analyzed by ELISA-based kits. **, $P < 0.01$ versus CO-treated cells. (B) NF-κB was analyzed by electrophoretic mobility shift assay. Protein–DNA complexes are shown. Arrowhead indicates nonspecific bands. (C) Nuclear extract was analyzed by immunoblotting for IRF-3 nuclear translocation, followed by stripping and reprobing for upstream stimulatory factor 2 (USF2).

macrophages (Fig. 3 D). On the other hand, as expected, the levels of LPS-induced TNF-α production were comparable in wild-type and *tlr3*$^{-/-}$macrophages (Fig. 3 D). Activation of both TLR3 and TLR4 signaling cascades induces IFN-β through the activation of IFN regulatory factor 3 (IRF-3), leading to the production of IFN-inducible gene products, such as IFN-γ–inducible protein 10 (IP-10) and the regulated upon activation, normal T expressed, and presumably secreted protein (RANTES; references 17 and 18). Although CO significantly inhibited LPS-induced IFN-β gene expression and the production of IP-10 and RANTES, the induction of these cytokines by poly(I:C) was not inhibited by CO (Fig. 4, A and B).

CO modulates transcription factor activation by TLR ligands, but not by poly(I:C)

Both NF-κB and IRF-3 are key transcription factors activated in TLR3 and TLR4 signaling pathways (7, 16). Because CO inhibited the TLR ligand–induced (except TLR3) cytokine production, we next examined the effect of CO on the ligand-induced activation of NF-κB and IRF-3. CO inhibited LPS-induced NF-κB activation as described previously (19), and Pam-, Fla-, and CpG-induced NF-κB activation was also significantly suppressed by CO (Fig. 5, A and B). Translocation of IRF-3 to the nuclear fraction increased after LPS treatment (18), and CO significantly suppressed its translocation (Fig. 5 C). However, CO had no effect on poly(I:C)-induced NF-κB activation and translocation of IRF-3 (Fig. 5). Consistent with the effect of CO on TLR ligand–induced cytokine production (Figs. 3 and 4), CO inhibited the activation of transcriptional factors by LPS, but not by poly(I:C) (Fig. 5). These results indicate that CO differentially regulates TLR signaling pathways.

CO suppresses the interactions of TLR4 and adaptor molecules

With the exception of TLR3, all the TLRs interact with an adaptor protein, MyD88 (7). TLR3 uses only the adaptor molecule TIR domain–containing adaptor-inducing IFN-β (TRIF) to activate IRF-3, and TLR4 also activates IRF-3 through TRIF. To investigate the effect of CO on upstream events in TLR signaling pathways, we assessed the effect of CO on interactions of TLRs and adaptor molecules that are subsequently induced after ligand binding to TLR (7, 8). We observed increased interaction not only between TLR4 and MyD88 but also between TLR4 and TRIF at 5 min after LPS treatment (20); however, CO markedly attenuated both interactions (Fig. 6 A). Although poly(I:C) treatment also increased the interaction of TLR3 and TRIF, CO did not suppress the TLR3 and TRIF interaction (Fig. 6 B). These experiments support the notion that the negative regulation of CO on TLR signaling pathways is likely to be dependent not on adaptor proteins, but on the specificity of TLRs.

CO regulates translocation of TLRs to lipid rafts

Membrane rafts are involved with TLR signaling, including the activation of NF-κB and cytokine production (11, 21). To further address the involvement of lipid rafts on TLR signaling pathways and the potential role of CO on the membrane rafts, cells were stimulated with LPS or poly(I:C)

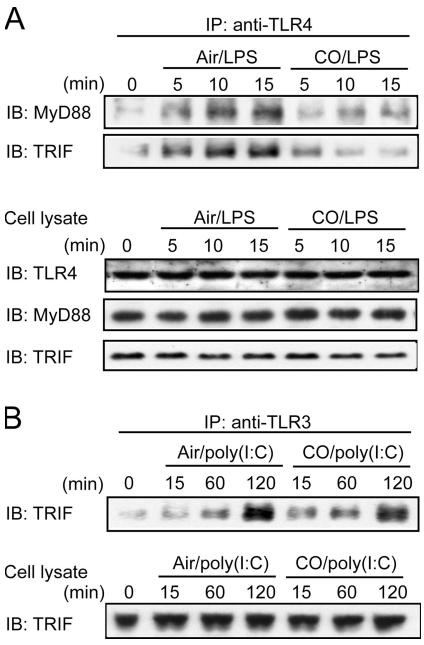

Figure 6. Effect of CO on interactions of TLRs and adaptor molecules. RAW 264.7 cells were treated with 100 ng/ml LPS or 20 μg/ml poly(I:C) in the absence or presence of CO. (A) Interaction between TLR4 and MyD88 or TLR4 and TRIF was analyzed with immunoprecipitation and immunoblotting. Expression of TLR4, MyD88, and TRIF was analyzed by immunoblotting using total cell lysates. (B) Interaction of TLR3 and TRIF was analyzed with immunoprecipitation and immunoblotting.

in the presence or absence of CO and incubated with FITC–cholera toxin (CTx). CTx specifically binds to the glycosphingolipid 1 (GM1), which is enriched in lipid rafts (22, 23). In the resting RAW 264.7 cells, the distribution of GM1 on the plasma membrane was quite homogeneous and TLR4 localized, in a diffuse manner, both in the membrane and intracellular compartment (Fig. 7 A; reference 21). After LPS treatment, a large fraction of TLR4 translocated to the plasma membrane, and colocalization of TLR4 and GM1 was also observed (Fig. 7 A). In CO-treated cells, the LPS-induced translocation of TLR4 to the membrane rafts was significantly inhibited (Fig. 7 A). In contrast, TLR3 localized in the intracellular compartment in the resting cells (Fig. 7 A), which is consistent with previous results (17, 24), and remained unchanged after poly(I:C) stimulation, even when CO was added (Fig. 7 A). The localization of TLR4 and TLR3 did not change in the cells treated with CO alone (unpublished data). Next, cells were incubated with FITC-CTx and cross-linked with anti-CTx. CTx specifically binds to the GM, and GM1-CTx can be crossed-linked to membrane patches with anti-CTx (22, 23, 25). These membrane patches have properties that are similar to those of biochemically isolated rafts (22, 23, 25).Without anti-CTx cross-linking, distribution of GM1 on the plasma membrane was homogeneous and TLR4 was expressed in a diffuse manner (Fig. S1 A, available at http://www.jem.org/cgi/content/full/jem.20060845/DC1). After the anti-CTx cross-linking at 37°C, a large part of GM1 translocated to a crescent-shaped patched area in the plasma membrane and a large fraction of TLR4 also translocated to the same area. Colocalization of TLR4 and GM1 was observed (Fig. S1 A). In contrast, TLR3 remained unchanged in the cytosolic fraction, not in the crescent-shaped patched area, after the cross-linking at 37°C (Fig. S1 B). To further investigate whether CO modulates the translocation of TLR4 and its adaptor molecules to lipid rafts, we isolated raft fractions and examined the translocation of the proteins involved in TLR signaling by immunoblotting. Flotillin-1, constitutively expressed in lipid rafts (26), localized in fractions 3 and 4. LPS or CO treatment had no effect on its abundance among the sucrose density fractions (Fig. 7 B). Most of GM1 localized in the same fractions (Fig. 7 B) and no alteration of the distribution was observed by LPS or CO treatment (unpublished data; references 11 and 27). TLR4 and its adaptor molecules (MyD88 and TRIF), as well as MD-2, IL-1 receptor–associated kinase, TNF receptor–associated factor (TRAF)-6, p65, and IκB-α, rapidly translocated to lipid rafts after LPS stimulation (11, 27), whereas TRAF-2 was not translocated (Fig. 7 B). In contrast, CO significantly inhibited the LPS-induced recruitment of TLR4 and other signaling molecules to lipid rafts (Fig. 7 B). The distribution of TLR4 was not affected by CO treatment alone (Fig. 7 B). Consistent with other data (11), CD-14 was constitutively expressed mainly in lipid rafts of resting cells and its expression was unaffected by LPS or CO treatment (Fig. 7 B). To confirm the differential localization and translocation patterns of TLRs, TLR3, 4, and 9 were immunoprecipitated with each antibody and immunoblotted with the same antibody using Triton X-100 soluble and insoluble raft fractions. After the ligand stimulation, TLR4 and TLR9 translocated to the rafts fraction, whereas TLR3 did not (Fig. 7 C). In addition, the adaptor protein TRIF interacted with TLR4 in the rafts fraction by LPS stimulation, but not with TLR3 by poly(I:C) (Fig. 7 C). These results confirm the differential translocation of TLRs to lipid rafts by ligand stimulation and agree with our immunofluorescence data (Fig. 7 A and Fig. S1). To examine the role of lipid rafts as a platform of ligand-induced TLR activation, we pretreated cells with MβCD and stimulated them with LPS, Pam, or poly(I:C). Although LPS- or Pam-induced TNF-α production was significantly reduced by MβCD treatment, poly(I:C)-induced cytokine production was unaffected (Fig. 7 D; references 11 and 28). In contrast, pretreatment of monodansylcadaverine (MDC), an inhibitor of the clathrin-dependent internalization pathway (29), markedly suppressed TNF-α production by poly(I:C) treatment, but not by LPS or Pam in macrophages (Fig. 7 E). These data suggest that the involvement of lipid rafts in TLR signaling is dependent on the specificity of the TLRs.

Inhibition of ROS generation by CO suppresses trafficking of TLR to rafts

ROS are known to be critical in intracellular signaling, including the TLR signaling pathway, and the scavenging of ROS

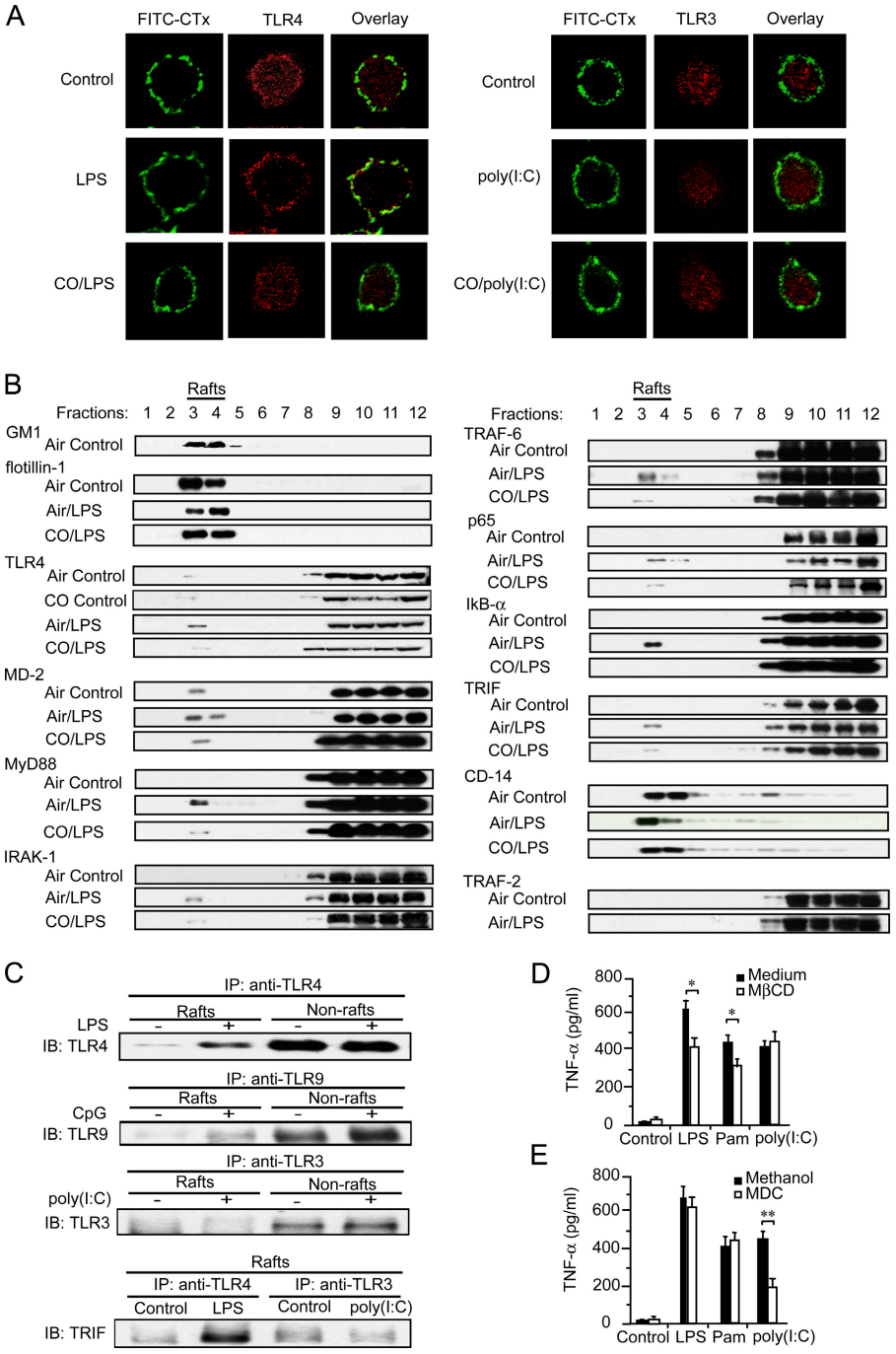

Figure 7. Lipid rafts are involved with TLR signaling, but not TLR3. (A) RAW 264.7 cells were stimulated with LPS or poly(I:C) in the presence or absence of CO for 1 h, followed by incubation of FITC-CTx on ice for 10 min. Cells were analyzed for FITC-CTx–stained GM1 (green) and TLR4 or TLR3 (red) by confocal microscopy. (B) RAW 264.7 cells were stimulated with LPS in the presence or absence of CO for 5 min. Cell lysates were fractionated by sucrose-gradient ultracentrifugation, followed by fractionation to 12 subfractions for immunoblotting with flotillin-1, TLR4, and other signaling proteins. (C) RAW 264.7 cells were treated with LPS, CpG, or poly(I:C) for 1 h, and then lipid raft fractions (fractions 3 and 4) and nonraft fractions (fractions 9–12) were separated. TLR3, 4, or 9 was immunoprecipitated with anti-TLR3, 4, or 9 mAb from raft fractions or nonraft fractions, followed by immunoblotting with the anti-TLR3, anti-TLR4, or anti-TRIF mAb. (D) RAW 264.7 cells were pretreated with 15 mM MβCD or medium for 15 min, followed by stimulation with LPS, Pam, or poly(I:C) for 1 or 2 h. Cell media were harvested and TNF-α production was analyzed by ELISA. *, $P < 0.05$ versus MβCD-treated cells. (E) RAW 264.7 cells were pretreated with 200 μM MDC or methanol as vehicle for 30 min, and then stimulated with LPS, Pam, or poly(I:C) for 1 or 2 h. TNF-α production in cell media was analyzed by ELISA. **, $P < 0.01$ versus MDC-treated cells.

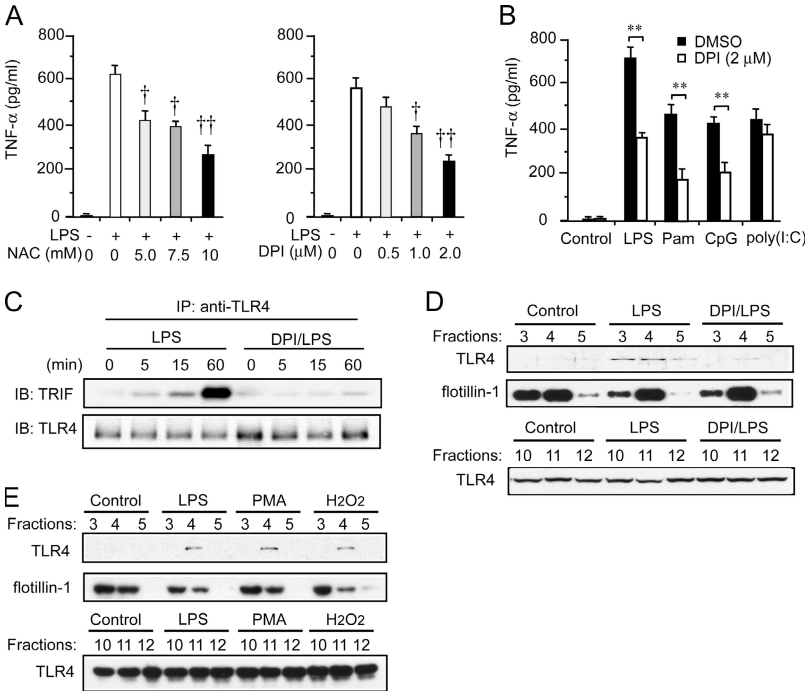

Figure 8. ROS generation is involved with translocation of TLR4 to lipid rafts. (A) RAW 264.7 cells were pretreated with the indicated concentration of NAC or DPI for 30 min, followed by incubation with LPS for 1 h. TNF-α production in cell media was analyzed by ELISA. †, $P < 0.05$ and ††, $P < 0.01$ versus LPS-treated control cells. (B) RAW 264.7 cells were pretreated with 2 μM DPI, followed by incubation with LPS, Pam, CpG, or poly(I:C) for 1 or 2 h. TNF-α production in cell media was analyzed by ELISA. **, $P < 0.01$ versus DPI-treated cells. (C) RAW 264.7 cells were pretreated with 2 μM DPI or DMSO as vehicle for 30 min, followed by incubation with 100 ng/ml LPS. Interaction between TLR4 and TRIF was analyzed with immunoprecipitation assay. (D and E) RAW 264.7 cells were pretreated with 2 μM DPI for 30 min, followed by incubation with 100 ng/ml LPS, 100 μM H_2O_2, or 1 μM PMA for 1 h. Cell lysates were fractionated to 12 subfractions, followed by immunoblotting for TLR4 and flotillin-1.

or the inhibition of NADPH oxidase suppresses LPS-induced cytokine production (30, 31). To examine if ROS are involved with the TLR signaling pathway and trafficking of TLR to lipid rafts, RAW 264.7 cells were pretreated with the antioxidant *N*-acetyl-L-cysteine (NAC) or a NADPH oxidase inhibitor, diphenylene iodonium (DPI), for 30 min, followed by incubation with TLR ligands. NAC and DPI suppressed LPS-induced TNF-α production in a dose-dependent manner (Fig. 8 A), and DPI significantly suppressed TNF-α production induced by LPS, Pam, and CpG, but not by poly(I:C) treatment (Fig. 8 B). DPI also inhibited LPS-induced interaction of TRIF and TLR4 (Fig. 8 C). In addition, we observed that the LPS-induced translocation of TLR4 to lipid rafts was inhibited by DPI treatment (Fig. 8 D). These results indicate that inhibition of NAPDH oxidase suppresses the TLR signaling pathway by modulating events upstream of the pathway. Furthermore, cellular stimulation with H_2O_2 and PMA also recruit TLR4 to lipid rafts (Fig. 8 E), which is consistent with previously reported results (32). To investigate the involvement of CO on TLR ligand–induced ROS generation, we detected TLR ligand–induced ROS production by using a fluorescence probe. CO significantly suppressed not only LPS- but also Pam-induced ROS production (Fig. 9 A). However, CO failed to inhibit poly(I:C)-induced ROS production in macrophages (Fig. 9 A). Upon stimulation, ROS are generated by NADPH oxidase, which forms a membrane-bound complex, including $p22^{phox}$ and $gp91^{phox}$ (cytochrome *b*558) and cytosolic proteins such as $p47^{phox}$ (33, 34). The complex of $gp91^{phox}$ and $p47^{phox}$ started to increase 5 min after LPS treatment, whereas complex formation was inhibited by CO as well as DPI treatment (Fig. 9 B). Furthermore, superoxide anion production, detected in isolated membrane fractions from LPS-treated macrophages, was inhibited when the cells were also exposed to CO (Fig. 9 C). Because CO is known to bind to heme proteins such as hemoglobin (1), we asked whether CO may interact with $gp91^{phox}$, a heme protein (34, 35). To address this question, we partially purified cytochrome *b*558 from bovine neutrophils and performed a spectral analysis. An oxidized spectrum was observed with a major peak at 410 nm. Heme proteins show major peak of absorption spectra typically at 400–450 nm and minor peaks in the range of 500–650 nm (35, 36). After incubation of the extract with sodium dithionite, the major peak shifted to 421 nm, generating distinct difference spectra (Fig. S2, available at http://www.jem.org/cgi/content/full/jem.20060845/DC1). Exposure of CO to the dithionite-reduced form of cytochrome *b*558 extract decreased the absorption peak and shifted the major peak from 421 to 418 nm, generating distinct

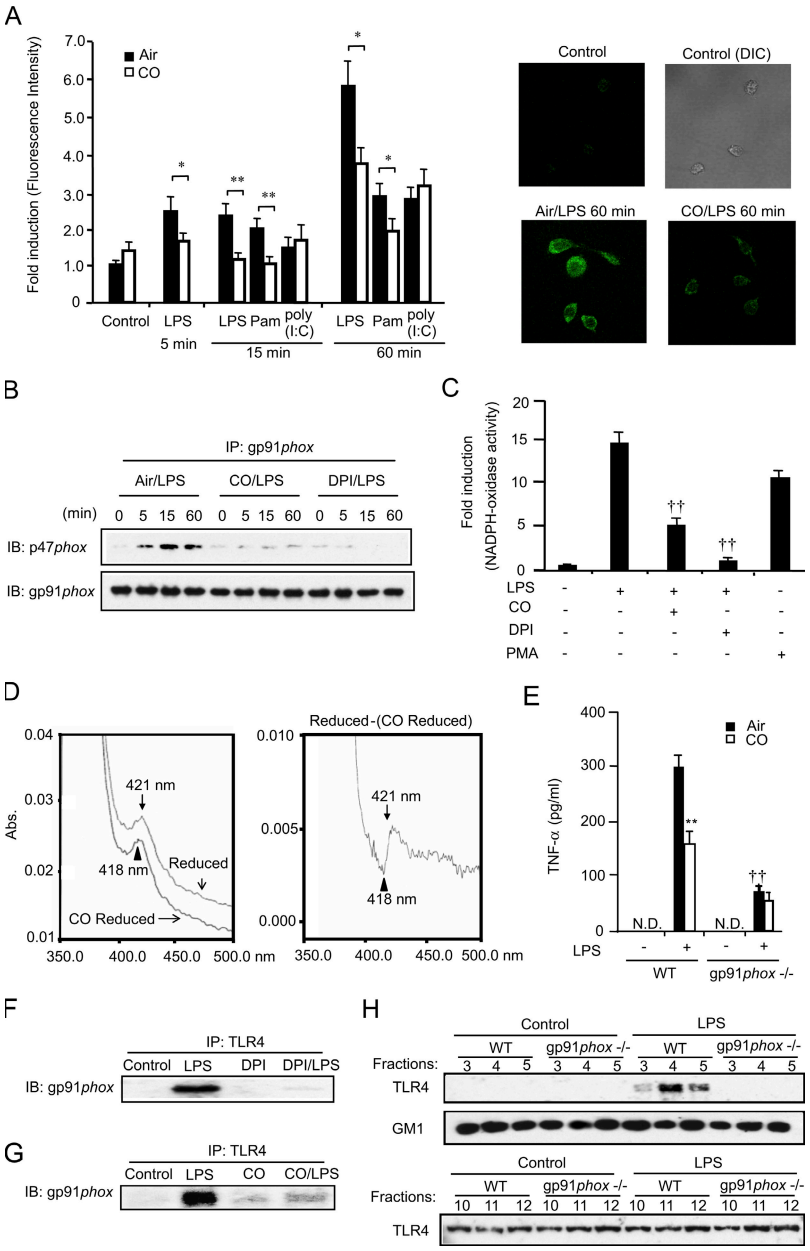

Figure 9. CO inhibits LPS-induced TLR4 trafficking by inhibiting NADPH oxidase activity. (A) RAW 264.7 cells were incubated with 100 ng/ml LPS, 100 ng/ml Pam, and 20 μg/ml poly(I:C) in the presence or absence of CO after preincubation with 10 μM CM-H_2DCFDA for 30 min. Fluorescence intensity of the cells was measured as the amount of ROS accumulation (left). Representative images are shown from three independent experiments (right). *, $P < 0.05$ and **, $P < 0.01$ versus CO-treated cells. (B) RAW 264.7 cells were treated with LPS in the presence or absence of CO or DPI. Interaction of gp91^{phox} and p47^{phox} was analyzed by immunoprecipitation assay. (C) RAW 264.7 cells were treated with LPS for 30 min in the presence or absence of CO or DPI. Superoxide production was analyzed by determining the reduction rate of acetylated cytochrome C. ††, $P < 0.01$ versus LPS-treated control cell. (D) Cytochrome *b*558 fraction was isolated from bovine neutrophils and the spectra of cytochrome *b*558 were analyzed. The isolated oxidized cytochrome *b*558 was reduced by adding 5 mM of sodium dithionite and CO was bubbled for 30 s, followed by spectra analysis (left). The spectral difference between the control (Reduced form) and CO-treated sample (CO Reduced) was shown (right). (E) Peritoneal macrophages were isolated from gp91^{phox}-deficient (gp91$^{phox-/-}$) mice and wild-type (WT) mice. Cells were exposed to LPS for 1 h in the presence or absence of CO. TNF-α production in cell media was analyzed by ELISA. ††, $P < 0.01$ versus air/LPS (WT). **, $P < 0.01$ versus air/LPS (WT). (F and G) RAW 264.7 cells were stimulated with LPS in the presence or absence of DPI or CO, and the interaction of TLR4 and gp91^{phox} was analyzed using immunoprecipitation assay. (H) Peritoneal macrophages from gp91^{phox}-deficient and wild-type mice were stimulated with 100 ng/ml LPS for 5 min. Cell lysates were fractionated to 12 subfractions, followed by immunoblotting for TLR4 and GM1.

difference spectra (Fig. 9 D). To elucidate the functional role of NADPH oxidase in TLR signaling, peritoneal macrophages from gp91^{phox}-deficient (gp91$^{phox-/-}$) mice were exposed with LPS in the presence or absence of CO. Cells from gp91$^{phox-/-}$ mice significantly produced less TNF-α in response to LPS than the cells from the wild-type control (37). The effect of CO on LPS-induced TNF-α production was impaired in gp91^{phox}-deficient cells (Fig. 9 E). In addition, we examined the interaction of TLR4 and gp91^{phox} by LPS. TLR4 interacted with gp91^{phox} in response to LPS treatment, whereas DPI treatment inhibited the interaction (Fig. 9 F). CO inhibited the LPS-induced complex formation of TLR4 and gp91^{phox} (Fig. 9 G). Finally, to confirm if NADPH oxidase is involved in the LPS-induced translocation of TLR4 to lipid rafts, we isolated lipid rafts from peritoneal macrophages from gp91$^{phox-/-}$ mice. TLR4 translocated to lipid rafts 5 min after LPS treatment in the wild-type cells; however, the translocation of TLR4 by LPS was suppressed in gp91^{phox}-deficient cells (Fig. 9 H). These results suggest that gp91^{phox} is involved with LPS-induced translocation of TLR4 to lipid rafts and that the effect of CO on trafficking to lipid rafts is potentially mediated by the modulation of gp91^{phox} and the suppression of NADPH oxidase activity, leading to the inhibition of trafficking of TLR4 to lipid rafts.

DISCUSSION

Although several negative regulators of TLR signaling have been reported (8), there are few reports that the modulation of TLR trafficking to lipid rafts correlates with the regulation of TLR signaling, and that elucidate the mechanism of trafficking (27). Here we demonstrate that TLRs show differential patterns of trafficking after TLR ligand stimulation, and that NADPH oxidase is critically involved with translocation of TLR4 to lipid rafts and downstream TLR signaling. Our results showed that TLR4 translocated to lipid rafts by LPS, whereas TLR3 remained in the intracellular compartment after poly(I:C) treatment. In addition, CO significantly suppressed LPS-induced ROS generation, resulting in the inhibition of the recruitment of TLR4 to the rafts and of downstream pathways, including activation of transcription factors and cytokine production. In contrast, CO failed to regulate the TLR3 signaling pathway. Thus, CO differentially regulated TLR signaling pathways.

CO negatively regulated TLR2, 4, 5, and 9 signaling pathways as revealed by the inhibition of cytokine production and the inactivation of transcription factors (Figs. 3–5). In addition, the effect of CO was exerted at the initial signaling events, TLR4–MyD88 or TLR4–TRIF complex formation (Fig. 6). In contrast, CO had no effect on poly(I:C)-induced TLR3 signaling pathways from complex formation of TRIF and TLR3 to cytokine production (Figs. 3–6), which is consistent with the observation that HO-1–overexpressing cells failed to suppress poly(I:C)-induced cytokine production (unpublished data). Although recent studies show that the cytoplasmic proteins RIG-I and MDA5 have also been identified as double-stranded RNA detectors (15, 38), our results demonstrate that TLR3 plays the dominant role in poly(I:C)-induced cytokine production at early time points in macrophages (Fig. 3 D; reference 16). It has been shown that several molecules act as negative regulators in multiple TLR signaling pathways and some of them exert their effects on the level of receptor or adaptor proteins (8). ST2 negatively regulates TLR2, 4, and 9, but not TLR3 signaling (39), which is similar with the differential effect of CO. Although ST2 suppresses TLR4 signaling by sequestration of the adaptor protein MyD88 and Mal, but not TRIF (39), CO inhibited the LPS-induced interaction of TLR4 and TRIF as well as of TLR4 and MyD88. Although Triad3A also negatively regulates TLR4- and TLR9-mediated signal activation, it has no effect on the TLR2 signaling pathway (40). Thus, the mechanism of negative regulation by CO on TLR signaling pathways is likely to be independent of the type of adaptor molecules as well as transcription factors, but dependent on the specificity of TLRs.

Our studies have shown that translocation of TLRs to lipid rafts is also dependent on their diversity (11, 12). Although IκB kinase α/β and IκB-α are recruited to the lipid rafts in B cell signaling (41), our data showed that LPS stimulation increased the trafficking of not only TLR4 but also other important signaling molecules in TLR signaling pathways to the raft membrane in macrophages (Fig. 7 B). This conclusion is supported by previous findings that MyD88 is translocated from cytosolic fraction to membrane fraction by LPS in RAW 264.7 cells (29). We showed that TRAF-6, a well-known important molecule in TLR signaling, translocated to the rafts 5 min after LPS stimulation, whereas TRAF-2 did not (Fig. 7 B). The differential trafficking patterns of TRAF-2 and TRAF-6 may be dependent on the specificity of ligand stimulation. In a similar fashion, CD40 engagement resulted in differential translocation patterns, such that TRAF-2 translocated to lipid rafts but TRAF-6 did not (42). We showed that CpG stimulation translocated TLR9 to membrane rafts (Fig. 7 C), similar to the previous observation that a small portion of TLR9 becomes cell surface accessible after CpG treatment (43). Together with previous results on the localization of TLR9 (43, 44), the recognition of CpG by TLR9 is likely to occur not only in the intracellular compartment but also in lipid rafts where TLR9 presumably clusters from cytosol after CpG stimulation in macrophages. Lipid rafts cross-linked with anti-CTx antibody immediately increase intracellular Ca^{2+}, which is up-regulated by ROS stimulation and which is required for the trafficking of molecules from the cytosolic compartment to the plasma membrane (32, 45, 46). Although cross-linking with anti-CTx causes signaling events analogous to activation of T cell receptor signaling (22, 23, 45), the results suggest that cross-linking by anti-CTx at 37°C is likely to provoke trafficking of TLR4 to the crescent-shaped membrane patch similar to biochemically isolated rafts. Although the cross-linking at 37°C showed translocation of TLR4 to the crescent-shaped patched area, TLR3 remained in the intracellular compartment (Fig. S1, A and B). These diverse patterns of TLRs

trafficking by the cross-linking are very similar to those by TLR ligand stimulation (Fig. 7, A and C). Moreover, the effect of MβCD and MDC on poly(I:C)-induced TNF-α production was opposite to the responses to LPS or Pam (Fig. 7, D and E). The signaling events of TLR3 are unlikely to occur in the raft membrane (17, 24), whereas the rafts are involved with the other TLR signaling pathways (11, 12).

Despite several results about the involvement of ROS in TLR signaling (30, 31), the role of ROS on trafficking to lipid rafts and on TLR signaling is still unclear. ROS such as superoxide or hydrogen peroxide are known to regulate activation of NF-κB or cytokine production (30, 31). We showed that LPS-induced NADPH oxidase–dependent ROS generation is critically involved in the translocation of TLR4 to lipid rafts and the initiation of the TLR signaling pathway. Furthermore, not only stimulation with hydrogen peroxide but also PMA, a potent NADPH oxidase activator (Fig. 9 C), can recruit TLR4 to lipid rafts (Fig. 8 E). Powers et al. (32) have reported that oxidative stress induced by hemorrhagic shock recruits TLR4 to the plasma membrane in macrophages. The present study shows that NADPH oxidase–dependent ROS generation induced by TLR ligand stimulation plays a critical role in the trafficking of TLR to lipid rafts and the initiation of downstream signaling pathways. In addition, the results suggest that the inhibitory effect of CO on the translocation of TLR4 to membrane rafts and on TLR signaling is mediated through the inhibition of NADPH oxidase activity. We observed similar differential effects of DPI and CO on TLR ligand–induced TNF-α production (Figs. 3 A and 8 B). In addition, we showed that CO significantly inhibited ROS production induced by LPS (47) and Pam, but not by poly(I:C), which is similar to the above data (Figs. 3 A and 9 A). Two integral membrane proteins, gp91^{phox} and p22^{phox}, form a stabilizing complex, termed cytochrome *b*558, and heme incorporation into gp91^{phox} is essential for the heterodimer formation (34). Recent studies showed that CO modulates the activity of heme proteins such as a potassium channel and soluble guanylate cyclase (1, 35, 48). Our spectral results also suggest that CO may form a complex with cytochrome *b*558 (Fig. 9 D). One of the critical roles of NADPH oxidase in professional immune cells is to generate ROS as a defense against invading microorganisms. It is known that gp91^{phox}-deficient humans, such as patients with chronic granulomatous disease, lack the ability to produce ROS, including superoxide (34). Our data showed that LPS-induced TNF-α production was significantly suppressed in macrophages from gp91^{phox}-deficient mice. In addition to this physiological importance of gp91^{phox} on LPS-induced proinflammatory cytokine production, we demonstrated LPS-induced interaction between gp91^{phox} and TLR4 by using immunoprecipitation analysis (Fig. 9 F). DPI, an NADPH oxidase inhibitor, suppressed this interaction as well as inhibited LPS-induced TLR4 signaling and cytokine production (Fig. 8, A–C). These results confirm a crucial link between gp91^{phox} and TLR4 signaling pathways. Consistent with previous results (47, 49), we showed that CO inhibits LPS-induced superoxide generation, associated with NADPH oxidase activation, in the membrane fraction of macrophages (Fig. 9 C). Furthermore, our results indicate that CO inhibited LPS-induced complex formation of gp91^{phox} and p47^{phox}, which is essential for assembling the active complex of NADPH oxidase (Fig. 9 B). The possible interaction of CO with cytochrome *b*558 may inhibit complex formation with cytosolic NADPH oxidase components. We showed that not only inhibition of NADPH oxidase activity but also lack of gp91^{phox} abolished the trafficking of TLR4 to the rafts by LPS (Figs. 8 D and 9 H). These results suggest that CO inhibits LPS-induced translocation of TLR4 to lipid rafts by inhibiting NADPH oxidase activity. Moreover, our results indicate that CO is likely to modulate gp91^{phox}, which is supported by the following observations: CO failed to suppress LPS-induced TNF-α production in gp91^{phox}-deficient macrophages; CO inhibited LPS-induced complex formation of gp91^{phox} and TLR4; and CO can form a complex with *b*558 in vitro (Fig. 9, D, E, and G).

Negative regulation of TLR signaling pathways by CO is likely to be mediated by the modulation of trafficking of TLRs to membrane rafts, and CO inhibits the trafficking by inhibition of NADPH oxidase activity, potentially through gp91^{phox}. First, CO suppressed TLR4 signaling, but not TLR3 (Figs. 3–6). Second, LPS stimulation rapidly translocated TLR4 to lipid rafts, but TLR3 did not translocate to the rafts in response to poly(I:C) as revealed by immunoblotting and immunofluorescence studies (Fig. 7, A–C). Third, CO blocked LPS-induced recruitment of TLR4 and other signaling molecules to lipid rafts (Fig. 7 B). Finally, CO suppressed LPS-induced ROS production including superoxide production (Fig. 9, A and C), and this effect of CO was impaired in gp91^{phox}-deficient cells (Fig. 9 E). Thus, ROS generated through NADPH oxidase activation is critically involved in signal transduction of TLRs in lipid rafts.

Recent studies in HO-1–deficient humans and mice provide the strongest evidence that HO-1 is a crucially important molecule in host defense against oxidative stress induced by various stimuli including LPS (2–4). Against invading PAMPs from microorganisms, macrophages dominantly contribute to the production of proinflammatory mediators (50). The high expression of TNF-α in the macrophages of HO-1$^{-/-}$ mice (Fig. 1) and negative regulatory effects of HO-1 on TLR ligand–induced TNF-α production in the macrophages (Fig. 2 A) suggest that HO-1 is likely to be an important molecule in regulating the activation of immune cells. Although biliverdin, the other byproduct of HO-1, also has cytoprotective effects (1), our results showed that scavenging CO by hemoglobin abolished the effect of HO-1 in TLR signaling (Fig. 2 B). Thus, HO-1 has a potent antiinflammatory role in TLR-mediated immune responses, and that role is mainly mediated through HO-1–derived CO (5, 14).

In summary, we have demonstrated that TLR trafficking evoked by ligand stimulation differentially occurred and that HO-1–derived CO negatively regulated TLR signaling pathways by the inhibition of TLRs trafficking to membrane rafts, resulting in suppression of downstream signaling

and cytokine production. In addition, CO inhibited trafficking of TLR by suppressing NADPH oxidase–dependent ROS generation. Because excessive inflammatory mediator production during sepsis causes severe tissue damage or organ dysfunction beyond essential host defense function (51), it is critically important to control ROS production as a key cell signaling activator in the immune system. The present study suggests that CO, a gas molecule produced physiologically in cells, might have a potent role to regulate PAMP-induced proinflammatory cascades by modulating ROS generation, resulting in the suppression of inappropriate hyperreactive immune responses. We have previously reported that the effect of CO on LPS-induced cytokine production is mediated by p38 MAPK (5), and recent results have suggested another mechanism of CO on the LPS-induced inflammatory response, which is mediated by PPAR-γ (52). However, these results do not address the involvement of MAPK and PPAR-γ in the trafficking of TLR to lipid rafts. Although further studies are needed to investigate the precise mechanisms of CO action, our results show that CO is a novel candidate as a negative regulator in TLR signaling pathways.

MATERIALS AND METHODS

Cell culture. RAW 264.7 cells and mouse peritoneal macrophages were maintained in DMEM containing 10% fetal bovine serum and antibiotics (5). For CO treatment, CO at a concentration of 1% corresponding to 10,000 ppm in compressed air was mixed with compressed air containing 5% CO_2 before delivery into the exposure chamber as described previously (5). After 2 h of pretreatment with either CO (0–500 ppm) or air, LPS (Sigma-Aldrich), peptidoglycan (Fluka), Pam_3CSK4 (InvivoGen), poly(I:C) (GE Healthcare), flagellin (InvivoGen), or CpG oligonucleotide was added to the culture media and the culture plates were returned to the chambers.

Transfection. RAW 264.7 cells were stably transfected with a pSFFV/HO-1 plasmid construct as described previously (5).

Mouse strains. C57BL/6 wild-type mice and $gp91^{phox}$-deficient mice (C57BL/6 background) were purchased from The Jackson Laboratory. HO-1–deficient mice were provided by S.-F. Yet (Brigham and Women's Hospital, Boston, MA; reference 53). TLR3-deficient mice were derived as described previously (54). Animals were housed according to guidelines from the American Association for Laboratory Animal Care and Research Protocols and were approved by the Animal Care and Use Committee (University of Pittsburgh School of Medicine).

Sucrose-gradient raft fraction. Sucrose-gradient raft fractions were separated as described previously (55). In brief, cells were lysed in ice-cold MBS buffer (25 mM MES, pH 6.5, 150 mM NaCl, 1% Triton X-100, 1 mM Na_3VO_4, and protease inhibitors). Lysates were adjusted to 4 ml of 40% sucrose by mixing with 2 ml of 80% sucrose and overlaid with 4 ml of 35% sucrose and 4 ml of 5% sucrose in MBS buffer. Samples were ultracentrifuged at 39,000 rpm for 18 h and fractionated into 12 subfractions.

Cytokine analysis. Media were analyzed with ELISA kits purchased from R&D Systems.

RNA quantification. Real-time PCR analysis was performed as described previously (56). mRNA expression was quantified by SYBR Green two-step, real-time RT-PCR for IFN-β. The sequence of the primer for IFN-β is 5′AGCTCCAAGAAAGGACGAACAT, 3′GCCCTGTAGGTGAGGTTGATCT (18). The expression of each gene was normalized to GAPDH mRNA content and calculated relative to control.

Electrophoretic mobility shift assay and NF-κB transcription factor assay. Nuclei extraction and electrophoretic mobility shift assay was performed as described previously (19). A double-stranded oligonucleotide containing the consensus transcription factor–binding site for NF-κB was purchased from Promega. p65 NF-κB transcriptional activity was also analyzed with ELISA-based kits purchased from Active Motif.

Immunoblotting and Immunoprecipitation. The rabbit anti-TLR4, TRAF-6, TRAF-2, IL-1 receptor–associated kinase 1, CD-14, and MD-2 were purchased from Santa Cruz Biotechnology, Inc. The rabbit anti-p65, total Iκ-B, and IRF-3 were purchased from Cell Signaling Technology. The rabbit anti-TRIF and TLR9 were purchased from Abcam. The rabbit anti-MyD88 was purchased from Chemicon. The rabbit anti-TLR3 and HO-1 were purchased from StressGen Biotechnologies. The mouse anti–flotillin-1, $p47^{phox}$, and $gp91^{phox}$ were purchased from BD Biosciences. CTx B Subunit peroxidase conjugate was purchased from Sigma-Aldrich. Immunoprecipitation and SDS-PAGE was performed as described previously (55, 57).

Immunofluorescence and confocal microscopy. After incubation with TLR ligands, the cells were washed with serum-free medium and incubated with 8 μg/ml FITC-conjugated CTx B (FITC-CTx; Sigma-Aldrich) on ice for 10 min. After fixation and permeabilization, cells were stained with the rabbit anti-TLR3 or anti-TLR4 (Santa Cruz Biotechnology, Inc.). After washing, samples were incubated with Alexa 594–coupled secondary antibody for 1 h (55). For raft-aggregation experiments, cells were incubated with 8 μg/ml FITC-CTx on ice for 10 min, followed by incubation with 4 μl/ml goat anti-CTx (Calbiochem) for 15 min at 4 or 37°C (23). Cells were placed on ice and washed with cold PBS and then fixed, permeabilized, and stained with anti-TLR3 or anti-TLR4, as described above. For analyzing ROS, the cells were preincubated with 10 μM CM-H_2DCFDA (Invitrogen) for 30 min, followed by incubation with TLR ligands (31). Samples were viewed with an Olympus Fluoview 300 Confocal Laser Scanning head with an Olympus IX70 inverted microscope, as described previously (55). Fluorescence intensity of cells exposed with CM-H_2DCFDA was analyzed by Olympus Fluoview (V. 3.1.16) software from Olympus Optical Co.

Immunocytochemistry. Livers and kidneys were fixed, embedded, and serially sectioned (5 μm) in toto. Paraffin-embedded tissues were hydrated, retrieved, and immunostained with anti–TNF-α (BD Biosciences) and monoclonal anti–CI:A3-1(RDI) for macrophage staining. Bound primary antibodies were visualized with diaminobenzidine staining by using ABC kits (Vector Laboratories).

Preparation of membrane fraction and assay of superoxide anion production. Membrane fraction was isolated as described previously (58). The protein (1 mg/ml protein) was incubated with 1.2 mg/ml acetylated cytochrome C, 1 mg/ml NADPH in the presence or absence of 1 mg/ml superoxide dismutase for 20 min at 37°C. The reactions were read at 550 nm, subtracting the A550 of the reaction containing superoxide dismutase. The production of superoxide was calculated assuming an extinction coefficient of 21 mM^{-1} cm^{-1} for reduced cytochrome C and normalized for mg protein and reaction time. Values were expressed as fold increase over control value.

Cytochrome b558 isolation and spectral analysis. Fresh bovine peripheral blood was harvested and the neutrophils were isolated by using the erythrocyte-granulocyte fraction. Bovine cytochrome *b*558 was prepared as described previously (59). Isolated cytochrome *b*558 was analyzed on a double beam recording spectrophotometer (Shimadzu UV2501-PC). After determination of oxidized spectra, the sample cuvette was degassed and replaced with an atmosphere of argon. To obtain reduced spectra, the cuvette was injected through the septum with sodium dithionite solution

(5 mM). To obtain CO spectra, 100% CO was bubbled into the cuvette through a septum for 30 s. Corresponding difference spectra were digitally generated.

Statistical analysis. We performed statistical analysis by using an unpaired Student's *t* test. All Data are mean ± SD from three different experiments. We considered values of $P < 0.05$ to be statistically significant.

Online supplemental material. Fig. S1 shows the immunofluorescence image of TLRs after cross-linking with anti-CTx antibody in macrophages. Fig.S2 shows spectral analysis of cytochrome *b*558 isolated from bovine neutrophils. The online supplemental material is available at http://www.jem.org/cgi/content/full/jem.20060845/DC1.

We thank S. Li for providing technical information about CpG oligonucleotide, S.-F. Yet for providing HO-1–deficient mice, J. Peterson for assistance with the spectral analysis, and Emeka Ifedigbo for technical assistance.

A.M.K. Choi was supported by NIH P01HL070807, R01HL055330, R01HL060234, and R01HL079904. H.P. Kim was supported by AHA 0525552U. S.W. Ryter was supported by AHA 0335035N.

The authors have no conflicting financial interests.

Submitted: 21 April 2006
Accepted: 31 August 2006

REFERENCES

1. Ryter, S.W., D. Morse, and A.M. Choi. 2004. Carbon monoxide: to boldly go where NO has gone before. *Sci. STKE.* 2004:RE6.
2. Yachie, A., Y. Niida, T. Wada, N. Igarashi, H. Kaneda, T. Toma, K. Ohta, Y. Kasahara, and S. Koizumi. 1999. Oxidative stress causes enhanced endothelial cell injury in human heme oxygenase-1 deficiency. *J. Clin. Invest.* 103:129–135.
3. Poss, K.D., and S. Tonegawa. 1997. Reduced stress defense in heme oxygenase 1-deficient cells. *Proc. Natl. Acad. Sci. USA.* 94:10925–10930.
4. Kawashima, A., Y. Oda, A. Yachie, S. Koizumi, and I. Nakanishi. 2002. Heme oxygenase-1 deficiency: the first autopsy case. *Hum. Pathol.* 33:125–130.
5. Otterbein, L.E., F.H. Bach, J. Alam, M. Soares, H. Tao Lu, M. Wysk, R.J. Davis, R.A. Flavell, and A.M. Choi. 2000. Carbon monoxide has anti-inflammatory effects involving the mitogen-activated protein kinase pathway. *Nat. Med.* 6:422–428.
6. Morse, D., S.E. Pischke, Z. Zhou, R.J. Davis, R.A. Flavell, T. Loop, S.L. Otterbein, L.E. Otterbein, and A.M. Choi. 2003. Suppression of inflammatory cytokine production by carbon monoxide involves the JNK pathway and AP-1. *J. Biol. Chem.* 278:36993–36998.
7. Akira, S., and K. Takeda. 2004. Toll-like receptor signalling. *Nat. Rev. Immunol.* 4:499–511.
8. Liew, F.Y., D. Xu, E.K. Brint, and L.A. O'Neill. 2005. Negative regulation of toll-like receptor-mediated immune responses. *Nat. Rev. Immunol.* 5:446–458.
9. Dykstra, M., A. Cherukuri, H.W. Sohn, S.J. Tzeng, and S.K. Pierce. 2003. Location is everything: lipid rafts and immune cell signaling. *Annu. Rev. Immunol.* 21:457–481.
10. Manes, S., G. del Real, and A.C. Martinez. 2003. Pathogens: raft hijackers. *Nat. Rev. Immunol.* 3:557–568.
11. Triantafilou, M., K. Miyake, D.T. Golenbock, and K. Triantafilou. 2002. Mediators of innate immune recognition of bacteria concentrate in lipid rafts and facilitate lipopolysaccharide-induced cell activation. *J. Cell Sci.* 115:2603–2611.
12. Soong, G., B. Reddy, S. Sokol, R. Adamo, and A. Prince. 2004. TLR2 is mobilized into an apical lipid raft receptor complex to signal infection in airway epithelial cells. *J. Clin. Invest.* 113:1482–1489.
13. Chauveau, C., S. Remy, P.J. Royer, M. Hill, S. Tanguy-Royer, F.X. Hubert, L. Tesson, R. Brion, G. Beriou, M. Gregoire, et al. 2005. Heme oxygenase-1 expression inhibits dendritic cell maturation and proinflammatory function but conserves IL-10 expression. *Blood.* 106:1694–1702.
14. Lee, T.S., and L.Y. Chau. 2002. Heme oxygenase-1 mediates the anti-inflammatory effect of interleukin-10 in mice. *Nat. Med.* 8:240–246.
15. Meylan, E., and J. Tschopp. 2006. Toll-like receptors and RNA helicases: two parallel ways to trigger antiviral responses. *Mol. Cell.* 22:561–569.
16. Alexopoulou, L., A.C. Holt, R. Medzhitov, and R.A. Flavell. 2001. Recognition of double-stranded RNA and activation of NF-kappaB by Toll-like receptor 3. *Nature.* 413:732–738.
17. Kawai, T., and S. Akira. 2006. Innate immune recognition of viral infection. *Nat. Immunol.* 7:131–137.
18. Doyle, S., S. Vaidya, R. O'Connell, H. Dadgostar, P. Dempsey, T. Wu, G. Rao, R. Sun, M. Haberland, R. Modlin, and G. Cheng. 2002. IRF3 mediates a TLR3/TLR4-specific antiviral gene program. *Immunity.* 17:251–263.
19. Sarady, J.K., S.L. Otterbein, F. Liu, L.E. Otterbein, and A.M. Choi. 2002. Carbon monoxide modulates endotoxin-induced production of granulocyte macrophage colony-stimulating factor in macrophages. *Am. J. Respir. Cell Mol. Biol.* 27:739–745.
20. Medvedev, A.E., A. Lentschat, L.M. Wahl, D.T. Golenbock, and S.N. Vogel. 2002. Dysregulation of LPS-induced Toll-like receptor 4-MyD88 complex formation and IL-1 receptor-associated kinase 1 activation in endotoxin-tolerant cells. *J. Immunol.* 169:5209–5216.
21. Hornef, M.W., B.H. Normark, A. Vandewalle, and S. Normark. 2003. Intracellular recognition of lipopolysaccharide by Toll-like receptor 4 in intestinal epithelial cells. *J. Exp. Med.* 198:1225–1235.
22. Bi, K., Y. Tanaka, N. Coudronniere, K. Sugie, S. Hong, M.J. van Stipdonk, and A. Altman. 2001. Antigen-induced translocation of PKC-theta to membrane rafts is required for T cell activation. *Nat. Immunol.* 2:556–563.
23. Gaide, O., B. Favier, D.F. Legler, D. Bonnet, B. Brissoni, S. Valitutti, C. Bron, J. Tschopp, and M. Thome. 2002. CARMA1 is a critical lipid raft-associated regulator of TCR-induced NF-kappa B activation. *Nat. Immunol.* 3:836–843.
24. Matsumoto, M., K. Funami, M. Tanabe, H. Oshiumi, M. Shingai, Y. Seto, A. Yamamoto, and T. Seya. 2003. Subcellular localization of Toll-like receptor 3 in human dendritic cells. *J. Immunol.* 171:3154–3162.
25. Harder, T., P. Scheiffele, P. Verkade, and K. Simons. 1998. Lipid domain structure of the plasma membrane revealed by patching of membrane components. *J. Cell Biol.* 141:929–942.
26. Fessler, M.B., P.G. Arndt, S.C. Frasch, J.G. Lieber, C.A. Johnson, R.C. Murphy, J.A. Nick, D.L. Bratton, K.C. Malcolm, and G.S. Worthen. 2004. Lipid rafts regulate lipopolysaccharide-induced activation of Cdc42 and inflammatory functions of the human neutrophil. *J. Biol. Chem.* 279:39989–39998.
27. Triantafilou, M., K. Brandenburg, S. Kusumoto, K. Fukase, A. Mackie, U. Seydel, and K. Triantafilou. 2004. Combinational clustering of receptors following stimulation by bacterial products determines lipopolysaccharide responses. *Biochem. J.* 381:527–536.
28. Dai, Q., J. Zhang, and S.B. Pruett. 2005. Ethanol alters cellular activation and CD14 partitioning in lipid rafts. *Biochem. Biophys. Res. Commun.* 332:37–42.
29. Ahmad-Nejad, P., H. Hacker, M. Rutz, S. Bauer, R.M. Vabulas, and H. Wagner. 2002. Bacterial CpG-DNA and lipopolysaccharides activate Toll-like receptors at distinct cellular compartments. *Eur. J. Immunol.* 32:1958–1968.
30. Park, H.S., H.Y. Jung, E.Y. Park, J. Kim, W.J. Lee, and Y.S. Bae. 2004. Cutting edge: direct interaction of TLR4 with NAD(P)H oxidase 4 isozyme is essential for lipopolysaccharide-induced production of reactive oxygen species and activation of NF-kappa B. *J. Immunol.* 173:3589–3593.
31. Matsuzawa, A., K. Saegusa, T. Noguchi, C. Sadamitsu, H. Nishitoh, S. Nagai, S. Koyasu, K. Matsumoto, K. Takeda, and H. Ichijo. 2005. ROS-dependent activation of the TRAF6-ASK1-p38 pathway is selectively required for TLR4-mediated innate immunity. *Nat. Immunol.* 6:587–592.
32. Powers, K.A., K. Szaszi, R.G. Khadaroo, P.S. Tawadros, J.C. Marshall, A. Kapus, and O.D. Rotstein. 2006. Oxidative stress generated by hemorrhagic shock recruits Toll-like receptor 4 to the plasma membrane in macrophages. *J. Exp. Med.* 203:1951–1961.
33. Li, J.M., and A.M. Shah. 2002. Intracellular localization and preassembly of the NADPH oxidase complex in cultured endothelial cells. *J. Biol. Chem.* 277:19952–19960.
34. Sumimoto, H., K. Miyano, and R. Takeya. 2005. Molecular composition and regulation of the Nox family NAD(P)H oxidases. *Biochem. Biophys. Res. Commun.* 338:677–686.

35. Taille, C., J. El-Benna, S. Lanone, J. Boczkowski, and R. Motterlini. 2005. Mitochondrial respiratory chain and NAD(P)H oxidase are targets for the antiproliferative effect of carbon monoxide in human airway smooth muscle. *J. Biol. Chem.* 280:25350–25360.
36. Reinking, J., M.M. Lam, K. Pardee, H.M. Sampson, S. Liu, P. Yang, S. Williams, W. White, G. Lajoie, A. Edwards, and H.M. Krause. 2005. The Drosophila nuclear receptor e75 contains heme and is gas responsive. *Cell.* 122:195–207.
37. Peng, T., X. Lu, and Q. Feng. 2005. Pivotal role of gp91phox-containing NADH oxidase in lipopolysaccharide-induced tumor necrosis factor-alpha expression and myocardial depression. *Circulation.* 111:1637–1644.
38. Kato, H., O. Takeuchi, S. Sato, M. Yoneyama, M. Yamamoto, K. Matsui, S. Uematsu, A. Jung, T. Kawai, K.J. Ishii, et al. 2006. Differential roles of MDA5 and RIG-I helicases in the recognition of RNA viruses. *Nature.* 441:101–105.
39. Brint, E.K., D. Xu, H. Liu, A. Dunne, A.N. McKenzie, L.A. O'Neill, and F.Y. Liew. 2004. ST2 is an inhibitor of interleukin 1 receptor and Toll-like receptor 4 signaling and maintains endotoxin tolerance. *Nat. Immunol.* 5:373–379.
40. Chuang, T.H., and R.J. Ulevitch. 2004. Triad3A, an E3 ubiquitin-protein ligase regulating Toll-like receptors. *Nat. Immunol.* 5:495–502.
41. Su, T.T., B. Guo, Y. Kawakami, K. Sommer, K. Chae, L.A. Humphries, R.M. Kato, S. Kang, L. Patrone, R. Wall, et al. 2002. PKC-beta controls I kappa B kinase lipid raft recruitment and activation in response to BCR signaling. *Nat. Immunol.* 3:780–786.
42. Arron, J.R., Y. Pewzner-Jung, M.C. Walsh, T. Kobayashi, and Y. Choi. 2002. Regulation of the subcellular localization of tumor necrosis factor receptor–associated factor (TRAF)2 by TRAF1 reveals mechanisms of TRAF2 signaling. *J. Exp. Med.* 196:923–934.
43. Latz, E., A. Schoenemeyer, A. Visintin, K.A. Fitzgerald, B.G. Monks, C.F. Knetter, E. Lien, N.J. Nilsen, T. Espevik, and D.T. Golenbock. 2004. TLR9 signals after translocating from the ER to CpG DNA in the lysosome. *Nat. Immunol.* 5:190–198.
44. Leifer, C.A., M.N. Kennedy, A. Mazzoni, C. Lee, M.J. Kruhlak, and D.M. Segal. 2004. TLR9 is localized in the endoplasmic reticulum prior to stimulation. *J. Immunol.* 173:1179–1183.
45. Janes, P.W., S.C. Ley, and A.I. Magee. 1999. Aggregation of lipid rafts accompanies signaling via the T cell antigen receptor. *J. Cell Biol.* 147:447–461.
46. Qin, S., Y. Minami, M. Hibi, T. Kurosaki, and H. Yamamura. 1997. Syk-dependent and -independent signaling cascades in B cells elicited by osmotic and oxidative stress. *J. Biol. Chem.* 272:2098–2103.
47. Srisook, K., S.S. Han, H.S. Choi, M.H. Li, H. Ueda, C. Kim, and Y.N. Cha. 2006. CO from enhanced HO activity or from CORM-2 inhibits both O2- and NO production and downregulates HO-1 expression in LPS-stimulated macrophages. *Biochem. Pharmacol.* 71:307–318.
48. Jaggar, J.H., A. Li, H. Parfenova, J. Liu, E.S. Umstot, A.M. Dopico, and C.W. Leffler. 2005. Heme is a carbon monoxide receptor for large-conductance Ca2+-activated K+ channels. *Circ. Res.* 97:805–812.
49. Taille, C., J. El-Benna, S. Lanone, M.C. Dang, E. Ogier-Denis, M. Aubier, and J. Boczkowski. 2004. Induction of heme oxygenase-1 inhibits NAD(P)H oxidase activity by down-regulating cytochrome b558 expression via the reduction of heme availability. *J. Biol. Chem.* 279:28681–28688.
50. Jenner, R.G., and R.A. Young. 2005. Insights into host responses against pathogens from transcriptional profiling. *Nat. Rev. Microbiol.* 3:281–294.
51. Riedemann, N.C., R.F. Guo, and P.A. Ward. 2003. Novel strategies for the treatment of sepsis. *Nat. Med.* 9:517–524.
52. Bilban, M., F.H. Bach, S.L. Otterbein, E. Ifedigbo, J. de Costa d'Avila, H. Esterbauer, B.Y. Chin, A. Usheva, S.C. Robson, O. Wagner, and L.E. Otterbein. 2006. Carbon monoxide orchestrates a protective response through PPARgamma. *Immunity.* 24:601–610.
53. Yet, S.F., M.A. Perrella, M.D. Layne, C.M. Hsieh, K. Maemura, L. Kobzik, P. Wiesel, H. Christou, S. Kourembanas, and M.E. Lee. 1999. Hypoxia induces severe right ventricular dilatation and infarction in heme oxygenase-1 null mice. *J. Clin. Invest.* 103:R23–R29.
54. Rudd, B.D., J.J. Smit, R.A. Flavell, L. Alexopoulou, M.A. Schaller, A. Gruber, A.A. Berlin, and N.W. Lukacs. 2006. Deletion of TLR3 alters the pulmonary immune environment and mucus production during respiratory syncytial virus infection. *J. Immunol.* 176:1937–1942.
55. Kim, H.P., X. Wang, F. Galbiati, S.W. Ryter, and A.M. Choi. 2004. Caveolae compartmentalization of heme oxygenase-1 in endothelial cells. *FASEB J.* 18:1080–1089.
56. Nakao, A., K. Kimizuka, D.B. Stolz, J.S. Neto, T. Kaizu, A.M. Choi, T. Uchiyama, B.S. Zuckerbraun, M.A. Nalesnik, L.E. Otterbein, and N. Murase. 2003. Carbon monoxide inhalation protects rat intestinal grafts from ischemia/reperfusion injury. *Am. J. Pathol.* 163:1587–1598.
57. Wang, X., Y. Wang, J. Zhang, H.P. Kim, S.W. Ryter, and A.M. Choi. 2005. FLIP protects against hypoxia/reoxygenation-induced endothelial cell apoptosis by inhibiting Bax activation. *Mol. Cell. Biol.* 25:4742–4751.
58. Sekhar, K.R., P.A. Crooks, V.N. Sonar, D.B. Friedman, J.Y. Chan, M.J. Meredith, J.H. Starnes, K.R. Kelton, S.R. Summar, S. Sasi, and M.L. Freeman. 2003. NADPH oxidase activity is essential for Keap1/Nrf2-mediated induction of GCLC in response to 2-indol-3-yl-methylenequinuclidin-3-ols. *Cancer Res.* 63:5636–5645.
59. Quinn, M.T., C.A. Parkos, and A.J. Jesaitis. 1995. Purification of human neutrophil NADPH oxidase cytochrome b-558 and association with Rap 1A. *Methods Enzymol.* 255:476–487.